Pattern formation on the surface of the granular medium in a horizontal rotating cylinder filled with fluid

Veronika Dyakova *
Perm National Research Polytechnic University, Perm 614990, Russia and
Laboratory of Vibrational Hydromechanics, Perm State Humanitarian Pedagogical University, Perm 614990, Russia

Denis Polezhaev †
Laboratory of Vibrational Hydromechanics, Perm State Humanitarian Pedagogical University, Perm 614990, Russia

(Received 7 December 2021; accepted 4 April 2022; published 18 April 2022)

The stability of the interface between a low-viscosity fluid and a granular medium in a horizontal rotating cylinder is experimentally studied. We consider a moderate rotation when heavy granules are able to form an annular layer near a cylindrical wall under the action of centrifugal force. The gravitational force acting on the particles of the granular material fluidizes the granular bed and induces the rotation of the particles at the interface with a velocity different from that of the rotating fluid. The effect of gravity can be characterized by the ratio of the gravitational force to the inertial centrifugal force $\Gamma \equiv \frac{g}{(2\pi f)^2 a}$, and it increases with the decrease of the cylinder rotation rate. The observations revealed previously unobserved regular ripples at the interface in a narrow range of rotation rates. At a sufficiently low rotation rate, a large number of granules become suspended, and regular ripples disappear under the action of gravitational force. In the present study, the geometric characteristics and spatiotemporal dynamics of regular ripples are studied in a wide range of granular bed thickness, and a possible mechanism of the ripple formation is discussed.

DOI: 10.1103/PhysRevFluids.7.044302

I. INTRODUCTION

A rotating horizontal cylinder filled with fluid and/or granular medium is an example of an experimental setup that has been extensively used for investigation of a wide range of physical phenomena, such as traveling and standing waves, avalanches, segregation, and many others. Studies on flow regimes are fundamentally interesting and crucial for the optimization of industrial rotating devices used for mixing, drying, and milling and predicting debris flows, avalanches, etc.

The motion of a suspended dense granule in a rotating fluid is affected by two groups of forces: radial buoyancy and inertial centrifugal forces and vertical buoyancy and gravitational forces. The resultant radial force pushes suspended granules towards the rotating cylindrical wall so that these particles tend to form the annular layer. In the contrast, the resultant vertical force repels the granules from the surface of the annular layer. The disturbing effect of vertical (gravitational) force on the background of stabilizing (centrifugal) one can be estimated by the dimensionless acceleration

$$\Gamma \equiv g/(2\pi f)^2 a, \tag{1}$$

*dyakova@pspu.ru
†polezhaev@pspu.ru

where g is the acceleration of gravity and a is the distance from the rotation axis to the surface of axisymmetric granular layer.

When $\Gamma \ll 1$, the fluid and the annular layer of granular material rotate together with the cylinder. Nevertheless, Dyakova *et al.* [1] found that free surface waves initiate ripple formation at the interface between low-viscosity fluid and granular material in a rapidly rotating cylinder. When $\Gamma \gg 1$, the disturbing effect of gravity is great so that the annular granular layer collapses, and heavy granules tend to gather together near the bottom of the cylinder. The results of studying the multiphase flows in slowly rotating containers are described in detail in the review articles [2–4]. The present study concerns the case of a moderate rotation rate when $\Gamma \sim 1$. In this range of Γ, the disturbing gravitational force is of the same order of magnitude as the inertial centrifugal force.

On the other hand, multiphase systems related to rotating-drum configurations can be distinguished by the volume fractions of fluid and granular material. Earlier, a variety of pattern formation phenomena were observed in experiments with pure fluids in a very slowly rotating cylinder, e.g., u-shaped structures [5], shark teeth and fishlike patterns [6], hygrocysts [7], and some others.

Experimentalists inject small amounts of particles into flowing fluids to visualize their velocity fields, assuming that they do not disturb fluid flows. However, it was reported that some pure fluid rimming flows significantly differ from those observed in dilute suspensions. For example, particles that were initially uniformly distributed throughout the fluid were observed to redistribute themselves into equally spaced circumferential particle-rich regions separated by regions of fluid devoid of particles [8–10]. A similar effect was found for particles suspended at low volume concentration in a rotating horizontal cylinder completely filled with a low-viscosity fluid [11,12]. A theoretical explanation of the phenomenon suggests that the segregation occurs as a result of mutual interaction between the particles and inertial waves excited in the fluid.

In contrast to the mentioned studies, Konidena *et al.* [13] numerically studied radial and axial patterns of positively buoyant particles suspended in a viscous fluid. When $\Gamma \sim 1$, particles tend to form a core around the rotational axis. According to simulations, the cross section of the core is not circular but is of regular polygon geometry with various numbers of edges, including square, pentagon, and hexagon. A similar granular core geometry was obtained in experiments with a rapidly rotating cylinder ($\Gamma < 1$) by applying transverse oscillations [14]. It was assumed that the polygon geometry of the cross section is explained by the action of rotating waves with various azimuthal wave numbers excited under the conditions of the resonance frequency of the cylinder.

There is another limiting case when the volume of dry or wet granular medium is comparable in order of magnitude with the volume of a container. In rotating containers, binary mixtures tend to segregate. When a homogeneous binary granular mixture is placed in a two-dimensional (2D) rotating drum, radial segregation is observed. This is is a relatively fast process and occurs after a few revolutions of the drum. Depending on particle sizes and densities, radial streaks or a radial core can occur (see, for example, [15–17] or the recent review article [4]). In three-dimensional drums, where an axial transport of particles is possible, an initially homogeneous mixture will typically segregate into regular band patterns, where the concentration of one component is noticeably higher than that of the other components (see, for example, [18–20]). Axial segregation develops on a much longer timescale (hundreds or thousands of revolutions).

As particles flow along the cylindrical wall of a slowly rotating cylinder, this granular flow is similar to that seen on an inclined surface. Numerous studies concern the stability of monodisperse granular flows along slopes due to applications for geophysical situations: fingering instability observed during the propagation of a granular front [21], longitudinal vortices [22] and chevron-shaped traveling waves [23] in chute flows, and others.

The present study focuses on the pattern formation in a multiphase system consisting of a low-viscosity fluid and a granular medium that is is denser than the fluid. The volume of granular material varies widely and is comparable with the volume of the fluid. When the cylinder filled with both fluid and granular medium rotates rapidly about its horizontal axis the interface between the two phases is axisymmetric. When $\Gamma \sim 1$, gravitational force disturbs the interface and fluidizes the granular bed. The resulting suspension and pure fluid rotate at different rates. It is known that velocity difference

across the interface of two fluids provokes the onset of Kelvin-Helmholtz vortices [24,25]. These vortices are observed in many environments including oceans [26], clouds [27], volcanic density currents [28], and the magnetosphere [29].

It is important to note that the Kelvin-Helmholtz instability has a specific feature in a horizontal rotating container: The particles on the rising and the descending sides of the cylinder rotate at different angular velocities under the action of gravity, so that the oscillatory Kelvin-Helmholtz instability may develop. This type of instability has been studied for decades in the case of two layers of immiscible fluids with different densities and viscosities. Under horizontal oscillations, stably stratified layers of immiscible fluids are differentially accelerated due to their density contrast. If the fluids are contained in a container with end walls, the shear flow generated by oscillatory forcing consists of counterflowing layers, since the fluids are incompressible. This configuration was first examined by Wolf [30], who observed interface waves frozen in the frame of reference of the oscillating container. Later, Lyubimov and Cherepanov [31] examined the stability of superposed layers of inviscid fluids contained between horizontal oscillating plates. Their linear stability analysis yielded a dispersion relation analogous to the steady inviscid Kelvin-Helmholtz instability.

Subsequent studies of oscillating fluids were aimed at clarifying the role of viscosity. Experimental study [32] with fluids with large viscosity contrast (the ratio of viscosities was 100) showed a favorable agreement of measurements for the onset of interfacial instability with the inviscid theory [31]. Another group of authors [33–35] carried out both experiments and a linear stability analysis of immiscible fluids for a large range of viscosity contrasts. They reported that the inviscid model underestimates the threshold for fluids of equal viscosities but overestimates the threshold for fluids with a large viscosity contrast.

An alternative direction of research concerns the study of interfacial stability in the limit of low surface tension. One of the ways to reduce surface tension between fluids is to carry out experiments near the critical point. The experimental study [36] examined the liquid-vapor equilibrium of CO_2 near its critical point and found that the wavelength of the frozen Kelvin-Helmholtz waves is consistent with the theory [31]. Later, Gandikota *et al.* [37] carried out experiments on H_2 in order to study this instability when the temperature is varied near its critical point and also reported that the measured stability diagram agrees well with the inviscid theory.

Despite a detailed study of various multiphase flows in a wide range of dimensionless acceleration Γ and a broad range of observed phenomena, there remains a chance to detect new effects. In this study, we report experimental data on ripple formation at the interface between fluid and granular medium and discuss the obtained data in the assumption that the observed ripples are due to the oscillatory Kelvin-Helmholtz instability.

II. EXPERIMENTAL SETUP

The scheme of the experimental setup is shown in Fig. 1. It consists of a hollow transparent cylinder with an inner radius $R = 7.2$ cm and length $L = 2.2$ cm. The cylinder is filled with a water-glycerol solution carrying solid particles. According to preliminary experiments, regular ripples appear only if the interface is made up of a low-viscosity fluid and granules with a density slightly different from that of the fluid. For this reason, a low-viscosity aqueous glycerol solution and ion-exchange resin particles Lewatit S 1567 were used in the experiments. The kinematic viscosity $\nu =$ 3 cSt was measured by a capillary viscometer, and the fluid density $\rho_l = 1.10$ g/cm^3 was measured by a hydrometer. The diameter was determined by microscopy for a few hundred particles. The measurements were made both in the dry state and after immersion for several hours in water-glycerol solution. The mean particle diameter is 0.54 mm in the dry state and 0.60 mm in the solution. Particle density was measured by hydrostatic weighing: The density of dry particles is equal to 1.28 g/cm^3, and the density of wetted grains is 1.33 g/cm^3. Hereinafter, we will use the characteristics of only wetted grains, namely, $d_s = 0.60$ mm and $\rho_s = 1.33$ g/cm^3.

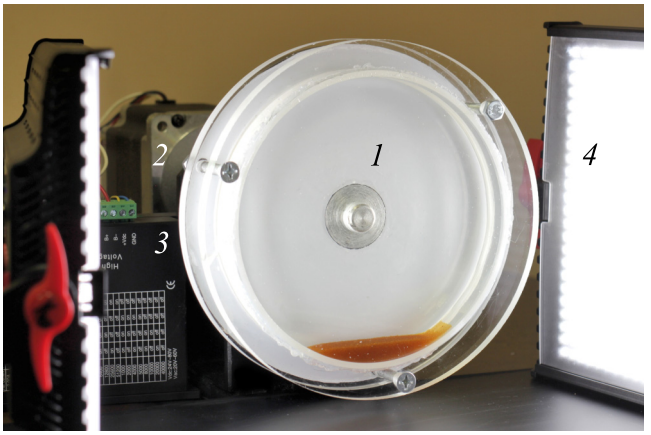

FIG. 1. Photo of the experimental setup

In a rapidly rotating cylinder, grains form an annular layer near the cylindrical wall of the cylinder. Therefore, it is convenient to characterize the amount of a granular medium by the thickness of the annular layer. In various experiments, the thickness h varied from 2 to 33 mm.

The cylinder *1* was supported by roller bearings and mounted on a massive horizontal platform. The stepper motor *2* was managed by the driver *3* and coupled to the cylinder and provided rotation about its horizontal axis with a rotation rate f up to 5 rps and accuracy of 0.05%. The rotating cylinder filled with water-glycerol solution and the granular medium was illuminated by two LED panels *4*.

In terms of dimensionless numbers, we have explored the following ranges: the dimensionless acceleration $\Gamma = g/(2\pi f)^2 a \in [0.3; 3]$, where $a = R - h$ is the distance from the rotation axis to the surface of the granular layer and the ratio of the thickness of the annular granular layer to the particle diameter $h/d_s \in [3; 55]$.

Each experiment followed a standard protocol. The cylinder was slowly accelerated from rest to several revolutions per second. After a solid body rotation was reached, the granular medium developed an annular layer near the cylindrical wall. Then, the rotation rate was slowly decreased with a step of 0.005 rps to 0.1 rps to determine the conditions required for the ripple formation. As soon as the axisymmetric sand surface became disturbed, photoregistration was initiated using a DSLR camera Canon EOS 60D and lenses Canon EF Lens 50 mm 1:1.8 STM.

It was also found that the ripples migrate along the cylindrical wall. The migration rate was measured with a high-speed camera CamRecord *CL*600×2 and lenses Nikon AF-S Nikkor 50 mm 1:1.4 G.

III. EXPERIMENTAL RESULTS

In a rapidly rotating cylinder, heavy granules form an axisymmetric annular layer near the cylindrical wall under the action of the centrifugal force [Fig. 2(a)]. With decreasing rotation rate, relief appears in the form of ripples with ridges oriented parallel to the axis of rotation [Fig. 2(b)]. According to the observations, a thin annular layer of the granular medium becomes completely fluidized, i.e., all granules can move relative to the cylinder. The ripples rotate together with the cylinder, wherein their shape depends on the azimuthal coordinate ϕ. The ripples are rather symmetric around the top point of the cylinder (azimuthal angle $\phi = 0$). On the descending (right) wall, the peaks of the ripples rotate faster than their bases, so that granules form vortices around the peaks. Then, the ripple slopes become symmetric around the bottom point of the cylinder ($\phi = \pi$). On the ascending (left) wall, the ripple height decreases, and the slopes become asymmetrical:

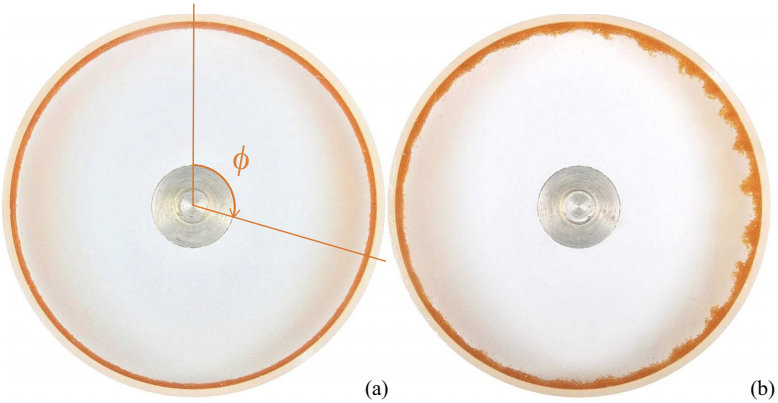

FIG. 2. Photograph of the granular medium in the cylinder rotating at different rates: $f = 3.50$ (a) and 1.15 (b) rps. The thickness of the granular bed $h = 2$ mm. The cylinder rotates clockwise.

gentle slopes face upward, and steep ones face downward. This effect becomes noticeable in the experiments with larger amounts of granular medium (Fig. 3).

In the experiments with a large number of granules, the granular bed is partially fluidized: The thickness of the fluidized layer increases with a decrease of the cylinder rotation rate. Regular ripples exist in a narrow range of f. At low rotation rates, a large number of granules become suspended, and the size of regular ripples increases significantly (Fig. 4). The suspended particles move erratically and unpredictably so that the shape of the ripples changes greatly during one revolution of the cylinder. However, the average number of ripples remains unchanged over several tens of minutes. For instance, number of ripples $N = 7$ and 8 for Figs. 4(a) and 4(b) respectively. At very low rotation rates, regular ripples disappear.

In the experiments with thick granular beds, we also added a small amount of white-colored granules in order to estimate the rotation rate of granules relative to the cylinder at different depths of the bed (see Figs. 3 and 4).

Visual examination of the ripples shows that their deformation is accompanied by a change in their azimuthal length. As shown in Fig. 5 the ripple length λ depends on the azimuthal coordinate ϕ: the ripple length takes a minimum value at an angle $\phi \approx 0$ and a maximum value at an angle $\pi/2 < \phi < \pi$. Hereinafter, we will use an average value of λ measured in the range $\pi/2 < \phi < \pi$ for comparison of experimental and theoretical data.

The change of the ripple azimuthal length within one revolution of the cylinder is an intriguing result. It can be explained if the ripples do not remain stationary relative to the cylinder but drift azimuthally. In order to study the spatiotemporal dynamics of the ripples, additional experiments were carried out using a high-speed camera. The frame rate was chosen in such a way that the cylinder rotated through an angle about one degree between successive frames. We measured the azimuthal coordinate of the peak of one ripple from each frame in a series of images. The results of the measurements are shown in Fig. 6. Each symbol in the figure represents the azimuthal coordinate of the ripple relative to the marker on the rotating cylinder in dependence on the dimensionless parameter tf (t is time). When $tf = 0, 1, 2, \ldots$ the marker is placed at the point with azimuthal coordinate $\phi = 0$. At that time, the azimuthal coordinate of the ripple peak closest to the marker location usually differs from zero, so $\Phi(tf)$ does not start from the origin. One can find that the instantaneous velocity of the ripple relative to the rotating cylinder is nonzero and changes periodically.

When the ripple starts to descend ($0 < \phi < \pi/2$ and $0 < tf < 0.25$), its azimuthal coordinate Φ slowly changes near the minimum. This means that the ripple rotates at about the same rate as the cylinder, i.e., the relative velocity of the ripple is close to zero. In the next quarter ($\pi/2 < \phi < \pi$

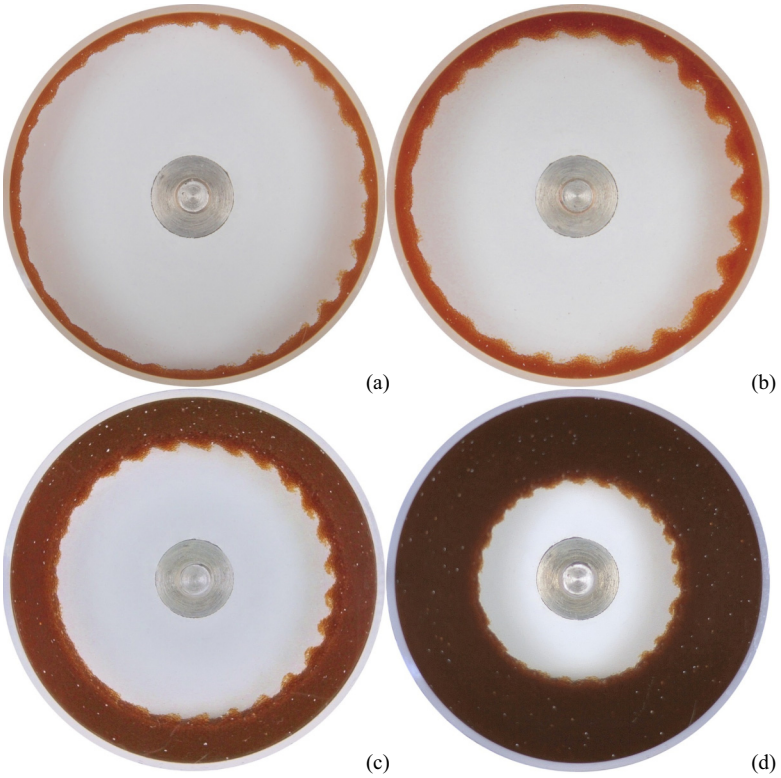

FIG. 3. Ripple formation obtained in the experiments with various amount of granular material: $h = 3$ mm and $f = 1.40$ rps (a), $h = 5$ mm and $f = 1.55$ rps (b), $h = 15$ mm and $f = 1.80$ rps (c), $h = 33$ mm and $f = 2.05$ rps (d). Reflection and absorption of light in the granular bed affects the visible color of the granules. The cylinder rotates clockwise.

and $0.25 < tf < 0.50$), coordinate Φ increases rapidly, therefore the ripple overtakes the cylinder. During the next quarter of a revolution, the increase of Φ slows down, then the coordinate reaches its maximum value and begins to decrease slowly. When $0.75 < tf < 1$, coordinate Φ decreases

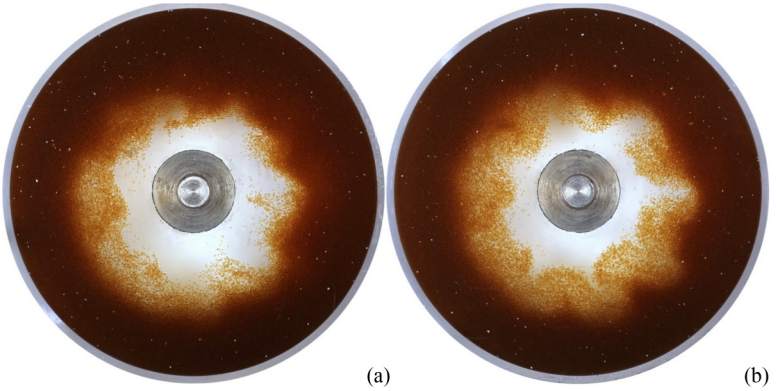

FIG. 4. Regular ripples containing large amount of suspended particles: $f = 1.47$ rps (a) and 1.50 rps (b); $h = 17$ mm. The cylinder rotates clockwise.

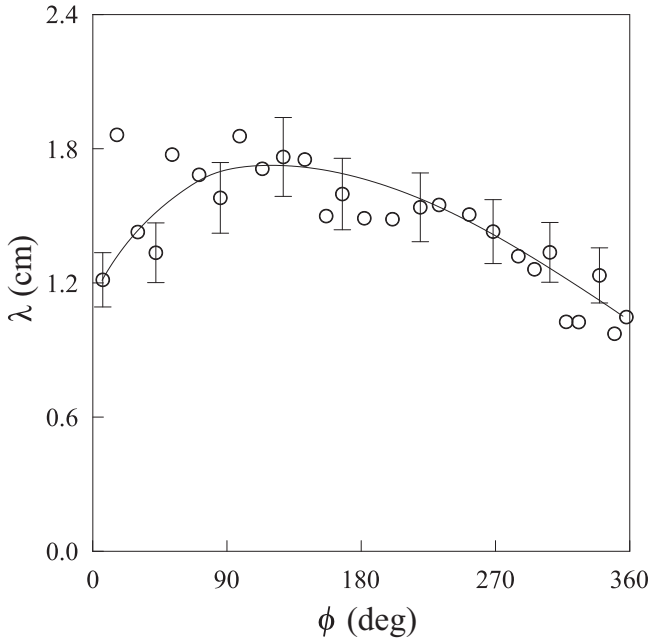

FIG. 5. Dependence of the ripple length λ on the azimuthal coordinate ϕ: $h = 2$ mm, $f = 1.2$ rps.

rapidly, therefore the ripple rotates slower than the cylinder. Thus, during one revolution, the ripples oscillate relative to the cylinder. A feature of this oscillatory motion is the fact that the azimuthal migration of the ripple in the phase of lagging rotation is greater than the azimuthal migration in the phase of advancing rotation. This is evidenced by the monotonic downward shift of $\Phi(tf)$.

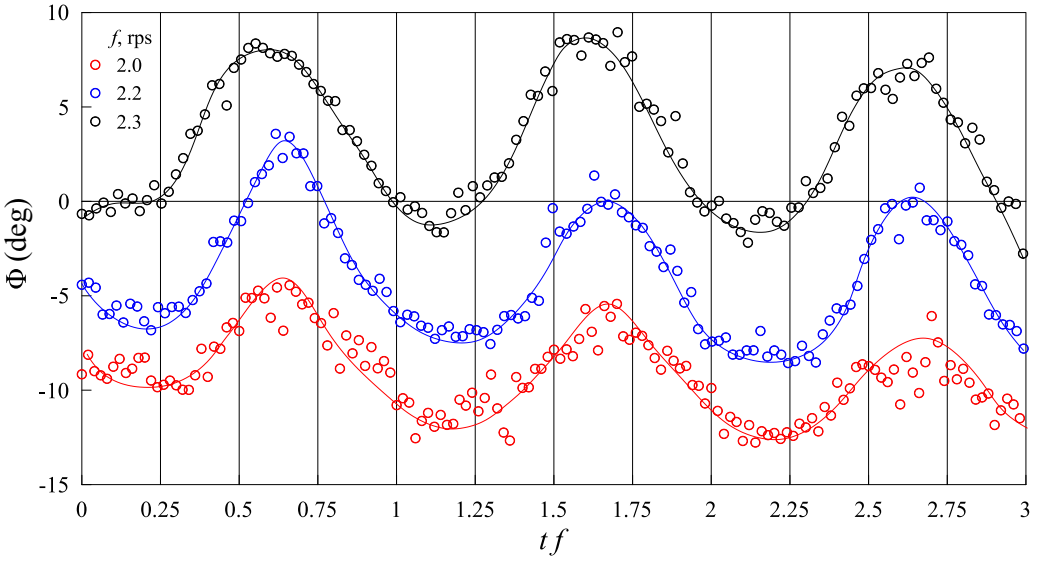

FIG. 6. Dependence of azimuthal coordinate Φ of a ripple relative to the rotating cylinder on dimensionless time tf for various rotation rates (h =33 mm).

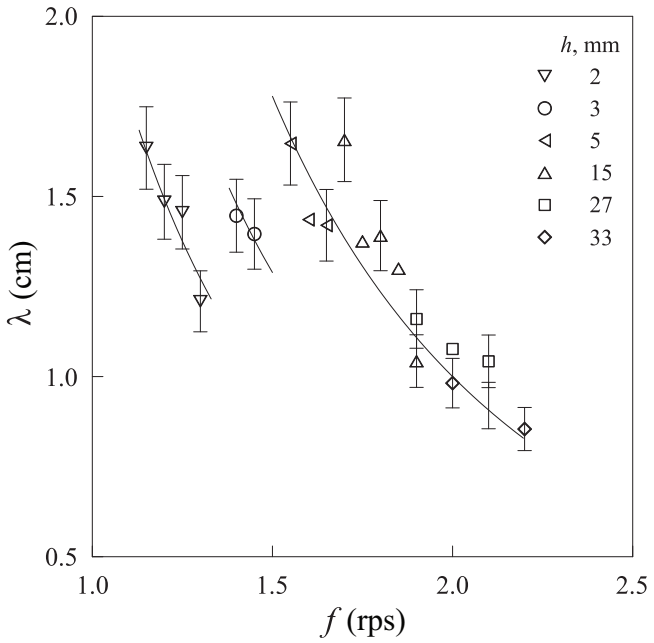

FIG. 7. Dependence of azimuthal length λ of granular ripples on rotation rate f of the cylinder for various thicknesses of granular bed.

Figure 7 reveals that the azimuthal length of the ripples slowly increases with decreasing rotation rate in the experiments with various amounts of granular material. What can be clearly seen in this figure is the good agreement of data obtained in the experiments with thick annular layers. In the limit of thin granular beds, the wavelength of ripples significantly differs from those of ripples observed at $h = 5$–33 mm.

IV. ANALYSIS OF EXPERIMENTAL DATA

In the previous section, it was illustrated that the fluidized granular medium oscillates relative to the rotating cylinder. Since the viscous fluid rotates at the same rate as the cylinder, the fluidized granular medium and pure fluid oscillate relative to each other. An important consequence of this is that the velocity difference across the interface between pure fluid and fluidized granular material can provoke the onset of the oscillatory Kelvin-Helmholtz instability.

Here we should note that shear instability is a known effect for granular flows. Various recent studies were devoted to the investigation of interfacial instabilities in bidisperse granular mixtures. For example, Ciamarra *et al.* [38] simulated the dynamics of a binary mixture of particles of different densities and revealed curl-like structures at the interface between shearing granular streams. A similar effect was experimentally observed at the interface between two streams of identical grains flowing on an inclined plane [39]. The authors stated that the interface waviness was driven by velocity shear instability. The formation of vortices at the granular flow–substrate interface is one more example of the Kelvin-Helmholtz-like instability [40]. Also, wavy patterns were revealed at the interface between two granular streams of different constant velocities on an inclined plane [41]. In a problem closer to that of the present investigation, Venditti and coauthors revealed transverse ripples on sand beds sheared by unidirectional currents in a series of flume experiments [42]. The authors found a good agreement between the observed wavelength and the wavelength predicted by the Kelvin-Helmholtz theory.

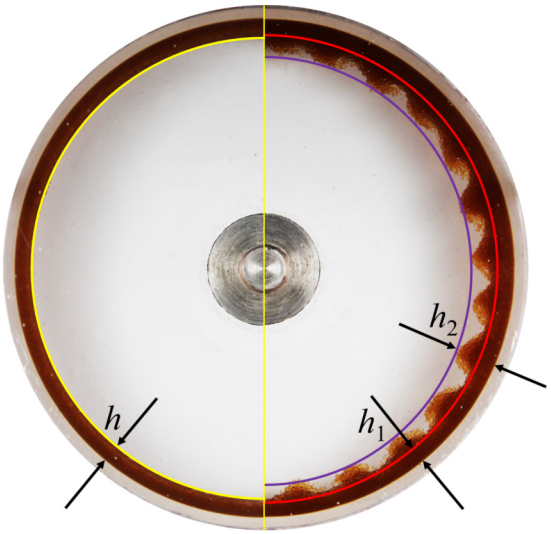

FIG. 8. Photo showing the thicknesses used to measure the porosity of the granular bed in the fluidized state: $h = 5$ mm, $f = 4$ rps (left) and 1.55 rps (right).

The present analysis is aimed at comparing the obtained experimental data on the ripple length and the wavelength of the expected shear instability. Here we will consider a fluidized granular medium and a low-viscosity water-glycerol solution as two immiscible fluids with zero surface tension. Lyubimov and Cherepanov [31] predicted that, in the limit of high frequencies $\omega = \frac{2\pi f H^2}{\nu} \gg 1$, the interface between two fluids becomes linearly unstable when

$$\Delta U^2 \geqslant \frac{\rho_s^2 - \rho_l^2}{\rho_s \rho_l} \frac{\lambda g}{\pi}, \tag{2}$$

where H is the height of regular ripples, ΔU is the velocity of the fluid relative to the fluidized granular medium, and g is the acceleration of gravity. This relation is analogous to the dispersion relation of the basic instability mode of steady Kelvin-Helmholtz type for two counterflows when $\Delta U/\sqrt{2}$ is regarded as the velocity difference in the classical case (see, for example, [43]).

Here we intend to evaluate the possibility of considering pure fluid and particles suspended in pure fluid as inviscid fluids. Many relations have been proposed for the dependence of the relative dynamic viscosity of suspensions μ_{rel} on solid fraction $c = 1 - P$, where P is the porosity of granular material, namely the ratio of pure fluid volume over the total volume of fluid and suspended particles. An overview of such relations can be found in [44]. According to these relations, the relative viscosity μ_{rel} depends only on solid fraction c and maximum solid fraction $c_{\max}$ of the particles. A often-used relation for the relative viscosity that does involve the maximum solid fraction $c_{\max}$ is given by Krieger and Dougherty [45]:

$$\mu_{\text{rel}} = (1 - c/c_{\max})^{-Bc_{\max}}, \tag{3}$$

where $B = 5/2$ for solid spherical particles. The maximum solid fraction $c_{\max} = 1 - P_{\min}$. This porosity is related to the porosity of the annular layer of the granular medium inside a rapidly rotating cylinder. When the granular medium is fluidized, its porosity increases. It is known from [46] that the porosity $P_{\min} = 0.4$ of granular medium consisting of randomly packed spheres, i.e., $c_{\max} = 0.6$.

The algorithm for evaluating the porosity P of the fluidized granular medium is as follows. First, we measured the thickness of the axisymmetric granular layer h (Fig. 8). Second, we determined the thickness of the nonfluidized granular layer h_1 in the quarter $\pi/2 < \phi < \pi$. Third, we calculated

the total thickness of the granular layer h_2 in the same quarter. Assuming that an initially densely packed column of particles with a height h extends to a column with a height h_2 in the presence of ripples and taking into account the conservation of mass inside a column of particles, one can obtain

$$h(1 - P_{\min}) = h_1(1 - P_{\min}) + (h_2 - h_1)(1 - P). \tag{4}$$

Finally, the porosity of the fluidized granular layer is

$$P = 1 - (1 - P_{\min})\frac{h - h_1}{h_2 - h_1}. \tag{5}$$

According to our calculations, the porosity varies in the range from 0.54 to 0.91 or, in other words, $c \in [0.09; 0.46]$ in the experiments. After substituting the obtained experimental values of c into Eq. (3) one can get that μ_{rel} varies in the range from 1.3 to 8.9. Then the dynamic viscosity of the suspension $\mu_{\text{sat}} = \mu_{\text{rel}}\nu\rho_l$ varies in the range from 4 to 29 mPa s.

Now we can calculate the kinematic viscosity of the fluid saturated with solid particles $\nu_{\text{sat}} = \mu_{\text{sat}}/\rho_{\text{sat}}$. When a fluid is saturated with solid particles, the density of suspension can be calculated by the following formula:

$$\rho_{\text{sat}} = \rho_s(1 - P) + \rho_l P. \tag{6}$$

Combining Eqs. (5) and (6) and rearranging them one can find

$$\rho_{\text{sat}} = \rho_l + (1 - P_{\min})(\rho_s - \rho_l)\frac{h - h_1}{h_2 - h_1}. \tag{7}$$

From our observations it follows that the density $\rho_{\text{sat}} \in [1.12; 1.22]$. Then, the kinematic viscosity ν_{sat} of the fluid saturated with solid particles changes from 4 to 24 cSt.

Finally, we can get the values of the dimensionless frequency for the aqueous solution of glycerol ω_l and for the suspension ω_{sat}. For typical values of the rotation rate $f = 1.5$ rps and the ripple height $H = 1$ cm, one can get $\omega_l = 314$ and $\omega_{\text{sat}} \in [39; 235]$. Regardless of the choice of the characteristic dimensionless frequency of oscillations, we can assume that $\omega \gg 1$, and we can use Eq. (2) to evaluate the experimental results.

The dispersion relation Eq. (2) can be rewritten taking into account the rotational motion of the ripples. First, $\Delta U = \frac{\Delta\Phi}{\Delta t}a = \Delta\omega a = 2\pi\Delta f a$, where a is the distance from the rotation axis to the undisturbed interface between the fluid and the porous medium, $\Delta\omega$ is the angular velocity of ripples relative to the fluid, and Δf is the rotation rate of the ripples. Second, we replace the acceleration of gravity, which indicates the downward action of gravity in the case of translational motion of two continuous media, with centrifugal acceleration, i.e., $g \to (2\pi f)^2 a$. Also, we introduce the relative density, defined as the ratio between the solid density and the fluid density, $\rho \equiv \frac{\rho_s}{\rho_l}$. We therefore write

$$\pi a \Delta f^2 \geqslant \left(\rho - \frac{1}{\rho}\right) f^2 \lambda. \tag{8}$$

We can rewrite Eq. (8) as follows:

$$\left(\frac{\Delta f}{f}\right)^2 \geqslant \left(\rho - \frac{1}{\rho}\right)\frac{\lambda}{\pi a}. \tag{9}$$

Let us introduce the notation $\Delta F \equiv (\frac{\Delta f}{f})$, which is the dimensionless rotation rate of the ripples, and the notation $\Lambda \equiv \frac{\lambda}{\pi a}$, which is the dimensionless ripple wavelength. Finally, we can rewrite the dispersion relation in the dimensionless form

$$\Delta F^2 \geqslant \left(\rho - \frac{1}{\rho}\right)\Lambda. \tag{10}$$

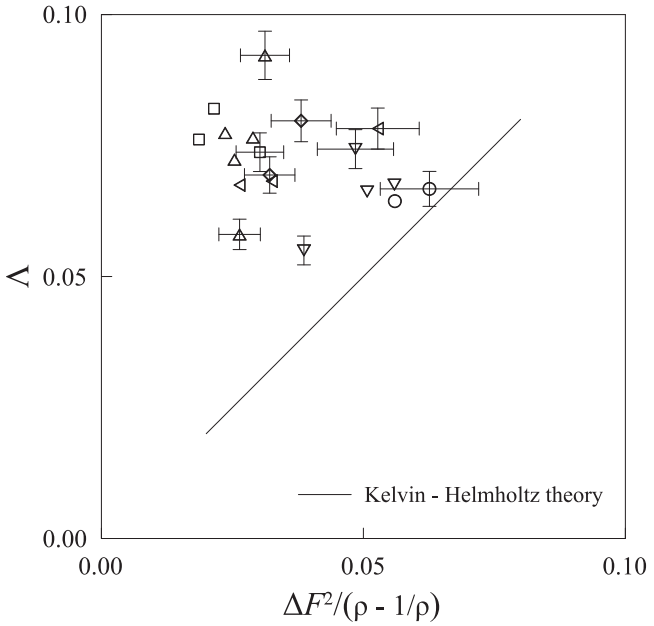

FIG. 9. Dependence of dimensionless length Λ of granular ripples on dimensionless parameter $\frac{\Delta F^2}{(\rho-\frac{1}{\rho})}$. The symbols correspond to those in Fig. 7. The solid line indicates the predictions of the theory of the oscillatory Kelvin-Helmholtz instability.

Thus, for a given frequency of the ripple rotation ΔF, the dimensionless wavelength of the Kelvin-Helmholtz waves can be evaluated from the formula

$$\Lambda \leqslant \frac{\Delta F^2}{\left(\rho - \frac{1}{\rho}\right)}. \tag{11}$$

To compare experimental data with theoretical predictions based on Eq. (2), the velocity of the ripple drift and the density of fluidized granular medium have to be examined. Since we calculated the ripple length λ in the range $\pi/2 < \phi < \pi$, the drift velocity

$$\Delta f = \frac{1}{2\pi}\frac{\Delta\Phi}{\Delta t} \tag{12}$$

should be measured in the same quarter. For this reason, we measured the slope of the tangent drawn to the curve $\Phi(t)$ for 3–5 successive revolutions of the cylinder and then calculated the average value of $\frac{\Delta\Phi}{\Delta t}$.

Figure 9 shows the results of comparing the wavelength, calculated by Eq. (2) using the known data on the velocity ΔF and the relative density ρ, and experimental data. The large horizontal error bars are explained by the uncertainty in measuring the thickness of the fluidized layer of the granular bed. Comparison of experimental results with theoretical predictions based on Eq. (2) shows that the data agree only in order of magnitude. A possible explanation for this fact is that dispersion relation was obtained in the limit of small disturbance amplitudes. Moreover, dispersion relation was deduced for a case of translational motion of two interacting fluids, but fluid and fluidized granular medium rotate in the present study. However, the results seem to be more positive for highly diluted suspensions ($\rho \to 1$ and $\frac{\Delta F^2}{(\rho-\frac{1}{\rho})}$ tends to the maximum value): the experimental data approach the theoretical line. This allows us to assert that the observed ripples appear due to the

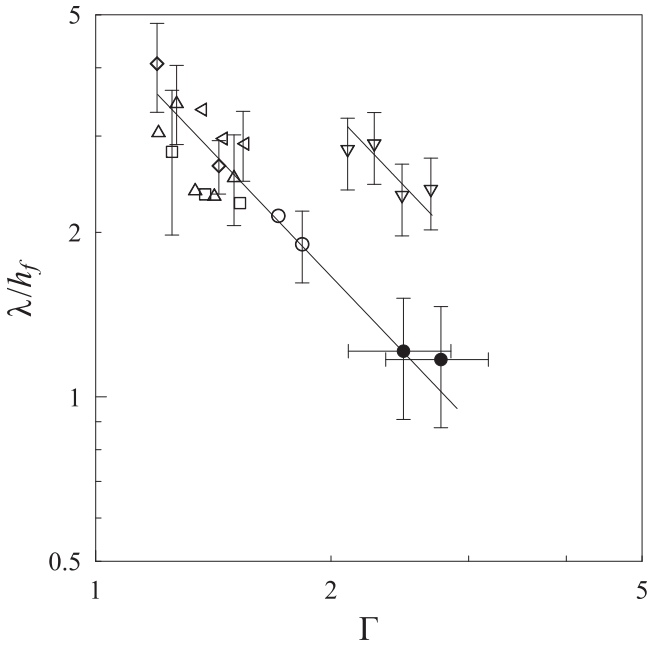

FIG. 10. Dependence of the ratio of the wavelength to the thickness of the fluidized layer of granular medium on the dimensionless acceleration. The empty symbols correspond to those in Fig. 7. The filled circles indicate the data obtained from Fig. 4.

oscillatory Kelvin-Helmholtz instability arising at the interface between pure fluid and fluidized granular medium.

Since the observed trend of experimental data does not agree well with the one predicted by Eq. (2), we should choose another parameter instead of $\frac{\Delta F^2}{(\rho-\frac{1}{\rho})}$ to determine the azimuthal wavelength of the observed Kelvin-Helmholtz waves. Since the ripples are due to the fluidization of granular material one can assume that the azimuthal size λ is determined by the thickness h_f of a fluidized layer. In turn, the fluidized layer thickness depends on the magnitude of the perturbations produced by the gravitational force. The effect of gravity can be estimated by the dimensionless acceleration $\Gamma = \frac{g}{(2\pi f)^2 a}$.

Figure 10 shows the dependence of the dimensionless wavelength of the observed Kelvin-Helmholtz waves $\frac{\lambda}{h_f}$ on the dimensionless acceleration Γ. The results of most experiments agree well with each other and therefore confirm the hypothesis that λ is determined by h_f. The large vertical error bars are explained by significant uncertainty in measuring the thickness of the fluidized layer of the granular medium.

Figure 10 also illustrates the results of measuring the length of ripples formed by a large number of suspended particles shown in Fig. 4 (filled circles). For these experimental symbols, the horizontal error bars are additionally shown since it is impossible to specify a single value of the distance a from the rotation axis to the suspended granules. The good agreement of the azimuthal size of the ripples consisting of suspended granules with the general trend in Fig. 10 confirms the hypothesis that the depth of the fluidized layer of granular medium determines the wavelength λ. At the same time, experimental data obtained in the experiments with a very thin layer of the granular material (inverted triangles in Fig. 10) disagree with the general trend. This is probably because the layer of the granular bed was too thin to form the required number of ripples for a given drift velocity. A similar effect was observed when studying ripple formation in a horizontal librating cylinder [47]. We speculate that the ripple length becomes "'satisfactory" when the parameter h/a reaches a critical

value. If so, then the critical value of dimensionless thickness is within the range from 0.028 to 0.042 ($2 < h < 3$ mm) in the present study.

V. SUMMARY

We have presented an experimental study of the phenomenon of pattern formation at the interface between the fluid and the granular medium in a horizontal rotating cylinder. We have found that gravitational force perturbs the surface of the granular medium and induces azimuthal oscillations of suspended granules relative to the rotating fluid. The velocity difference across the interface of two media provokes the onset of the Kelvin-Helmholtz instability. The analysis revealed that the experimental data on the azimuthal length of the observed ripples qualitatively agrees with the predictions of the oscillatory Kelvin-Helmholtz theory for two immiscible perfect fluids with zero surface tension. A more detailed analysis of the data suggests that the wavelength of the observed waves is determined by the thickness of the fluidized layer of the granular material, which increases as the disturbing effect of gravitational force grows stonger in comparison with the effect of centrifugal force.

Moreover, by using a high-speed camera we have shown that the observed ripples migrate relative to the rotating cylinder. This phenomenon has not been explained yet and needs further investigation.

In the present paper, we have not addressed the effect of the relative density ρ of two media and the granule diameter d_s on the ripple formation. We have started doing laboratory experiments using denser spheres of another diameter to complete our analysis. Another area of possible research includes a study of positively buoyant particles. Then, a granular medium will form a cylindrical column in the center of the rotating cell similar to that observed in [13]. The granular column will rotate relative to the fluid due to the action of gravitational force. We expect that the combined effect of relative rotation and proper relative density of granules will be able to excite Kelvin-Helmholtz waves.

ACKNOWLEDGMENTS

The authors are grateful to Prof. V. Kozlov for stimulating discussions during this work and careful reading of the manuscript. The work is supported by Grant No. 18-71-10053 of the Russian Science Foundation.

[1] V. Dyakova, V. Kozlov, and D. Polezhaev, Pattern formation inside a rotating cylinder partially filled with liquid and granular medium, Shock Vib. **2014**, 841320 (2014).

[2] G. Seiden and P. J. Thomas, Complexity, segregation, and pattern formation in rotating-drum flows, Rev. Mod. Phys. **83**, 1323 (2011).

[3] S. W. Meier, R. M. Lueptow, and J. M. Ottino, A dynamical systems approach to mixing and segregation of granular materials in tumblers, Adv. Phys. **56**, 757 (2007).

[4] P. B. Umbanhowar, R. M. Lueptow, and J. M. Ottino, Modeling segregation in granular flows, Annu. Rev. Chem. Biomol. Eng. **10**, 129 (2019).

[5] F. Melo, Localized states in a film-dragging experiment, Phys. Rev. E **48**, 2704 (1993).

[6] S. Thoroddsen and L. Mahadevan, Experimental study of coating flows in a partially-filled horizontally rotating cylinder, Exp. Fluids **23**, 1 (1997).

[7] R. Balmer and T. Wang, An experimental study of internal hygrocysts, J. Fluids Eng. **98**, 688 (1976).

[8] O. Boote and P. Thomas, Effects of granular additives on transition boundaries between flow states of rimming flows, Phys. Fluids **11**, 2020 (1999).

[9] D. D. Joseph, J. Wang, R.-y. Bai, B. H. Yang, and H. H. Hu, Particle motion in a liquid film rimming the inside of a partially filled rotating cylinder, J. Fluid Mech. **496**, 139 (2003).

[10] E. Guyez and P. J. Thomas, Spatiotemporal Segregation-Pattern Drift in Particle-Laden Rimming Flow, Phys. Rev. Lett. **100**, 074501 (2008).
[11] G. Seiden, M. Ungarish, and S. G. Lipson, Banding of suspended particles in a rotating fluid-filled horizontal cylinder, Phys. Rev. E **72**, 021407 (2005).
[12] E. Schwartz and S. G. Lipson, Banding oscillations of non-brownian particles in a rotating fluid, New J. Phys. **15**, 063036 (2013).
[13] S. Konidena, J. Lee, K. A. Reddy, and A. Singh, Particle dynamics and pattern formation in a rotating suspension of positively buoyant particles, Phys. Rev. Fluids **3**, 044301 (2018).
[14] A. Salnikova, N. Kozlov, A. Ivanova, and M. Stambouli, Dynamics of rotating two-phase system under transversal vibration, Microgravity Sci. Technol. **21**, 83 (2009).
[15] J. Gray and A. Thornton, A theory for particle size segregation in shallow granular free-surface flows, Proc. R. Soc. A **461**, 1447 (2005).
[16] G. Pereira, N. Tran, and P. Cleary, Segregation of combined size and density varying binary granular mixtures in a slowly rotating tumbler, Granular Matter **16**, 711 (2014).
[17] C. Liao, S. Hsiau, and H. Nien, Effects of density ratio, rotation speed, and fill level on density-induced granular streak segregation in a rotating drum, Powder Technol. **284**, 514 (2015).
[18] H. Kuo, R. Hsu, and Y. Hsiao, Investigation of axial segregation in a rotating drum, Powder Technol. **153**, 196 (2005).
[19] N. Taberlet, M. Newey, P. Richard, and W. Losert, On axial segregation in a tumbler: an experimental and numerical study, J. Stat. Mech.: Theory Exp. (2006) P07013.
[20] L. Naji and R. Stannarius, Axial and radial segregation of granular mixtures in a rotating spherical container, Phys. Rev. E **79**, 031307 (2009).
[21] O. Pouliquen, J. Delour, and S. B. Savage, Fingering in granular flows, Nature (London) **386**, 816 (1997).
[22] Y. Forterre and O. Pouliquen, Longitudinal Vortices in Granular Flows, Phys. Rev. Lett. **86**, 5886 (2001).
[23] S. L. Conway, D. J. Goldfarb, T. Shinbrot, and B. J. Glasser, Free Surface Waves in Wall-Bounded Granular Flows, Phys. Rev. Lett. **90**, 074301 (2003).
[24] S. W. Thomson, Hydrokinetic solutions and observations, London Edinburgh Dublin Philos. Mag. J. Sci. **42**, 362 (1871).
[25] H. von Helmholtz, Die energie der wogen und des windes, Ann. Phys. (Leipzig) **277**, 641 (1890).
[26] W. D. Smyth and J. N. Moum, Ocean mixing by Kelvin-Helmholtz instability, Oceanography **25**, 140 (2012).
[27] R. A. Houze, Jr., *Cloud Dynamics* (Academic, New York, 2014).
[28] J. Dufek, The fluid mechanics of pyroclastic density currents, Annu. Rev. Fluid Mech. **48**, 459 (2016).
[29] H. Hasegawa, M. Fujimoto, T.-D. Phan, H. Reme, A. Balogh, M. Dunlop, C. Hashimoto, and R. TanDokoro, Transport of solar wind into Earth's magnetosphere through rolled-up Kelvin–Helmholtz vortices, Nature (London) **430**, 755 (2004).
[30] G. H. Wolf, The dynamic stabilization of the rayleigh-taylor instability and the corresponding dynamic equilibrium, Z. Phys. A **227**, 291 (1969).
[31] D. Lyubimov and A. Cherepanov, Development of a steady relief at the interface of fluids in a vibrational field, Fluid Dyn. **21**, 849 (1986).
[32] A. Ivanova, V. Kozlov, and P. Evesque, Interface dynamics of immiscible fluids under horizontal vibration, Fluid Dyn. **36**, 362 (2001).
[33] E. Talib, S. V. Jalikop, and A. Juel, The influence of viscosity on the frozen wave instability: theory and experiment, J. Fluid Mech. **584**, 45 (2007).
[34] E. Talib and A. Juel, Instability of a viscous interface under horizontal oscillation, Phys. Fluids **19**, 092102 (2007).
[35] S. V. Jalikop and A. Juel, Steep capillary-gravity waves in oscillatory shear-driven flows, J. Fluid Mech. **640**, 131 (2009).
[36] R. Wunenburger, P. Evesque, C. Chabot, Y. Garrabos, S. Fauve, and D. Beysens, Frozen wave induced by high frequency horizontal vibrations on a CO_2 liquid-gas interface near the critical point, Phys. Rev. E **59**, 5440 (1999).

[37] G. Gandikota, D. Chatain, S. Amiroudine, T. Lyubimova, and D. Beysens, Frozen-wave instability in near-critical hydrogen subjected to horizontal vibration under various gravity fields, Phys. Rev. E **89**, 012309 (2014).
[38] M. P. Ciamarra, A. Coniglio, and M. Nicodemi, Shear Instabilities in Granular Mixtures, Phys. Rev. Lett. **94**, 188001 (2005).
[39] D. J. Goldfarb, B. J. Glasser, and T. Shinbrot, Shear instabilities in granular flows, Nature (London) **415**, 302 (2002).
[40] P. J. Rowley, P. Kokelaar, M. Menzies, and D. Waltham, Shear-derived mixing in dense granular flows, J. Sediment. Res. **81**, 874 (2011).
[41] A. Amon, R. Delannay, and A. Valance, *Shear instabilities in bidisperse granular flows, in Powders and Grains 2009: Proceedings of the 6th International Conference on Micromechanics of Granular Media*, 13–17 July 2009, Golden, CO, edited by M. Nakagawa and S. Luding, AIP Conf. Proc. No. 1145 (AIP, New York, 2009), pp. 583–586.
[42] J. G. Venditti, M. Church, and S. J. Bennett, On interfacial instability as a cause of transverse subcritical bed forms, Water Resour. Res. **42**, W07423 (2006).
[43] P. G. Drazin, *Introduction to Hydrodynamic Stability*, Cambridge Texts in Applied Mathematics Vol. 32 (Cambridge University Press, Cambridge, 2002).
[44] B. A. Horri, P. Ranganathan, C. Selomulya, and H. Wang, A new empirical viscosity model for ceramic suspensions, Chem. Eng. Sci. **66**, 2798 (2011).
[45] I. M. Krieger and T. J. Dougherty, A mechanism for non-Newtonian flow in suspensions of rigid spheres, Trans. Soc. Rheol. **3**, 137 (1959).
[46] J. von Seckendorff, K. Achterhold, F. Pfeiffer, R. Fischer, and O. Hinrichsen, Experimental and numerical analysis of void structure in random packed beds of spheres, Powder Technol. **380**, 613 (2021).
[47] D. Polezhaev, The geometry of sand ripples in a uniformly rotating and librating horizontal cylinder, Microgravity Sci. Technol. **32**, 807 (2020).